Supporting information for

A simple and cost-effective approach to fabricate tunable length polymeric microneedle patches for controllable transdermal drug delivery

Yongli Chen [a,b], Yiwen Xian [c], Andrew J. Carrier [d], Brian Youden [d,e], Mark Servos[e], Shufen Cui [c], Tiangang Luan[b], Sujing Lin[*], and Xu Zhang [d,*]

[a] Postdoctoral Innovation Practice Base, Shenzhen Polytechnic, Shenzhen, 518055, China.

[b] State Key Laboratory Biocontrol, School of Marine Sciences, Sun Yat-sen University, Guangzhou 510275, China.

[c] Department of Biological Applied Engineering, Shenzhen Key Laboratory of Fermentation Purification and Analysis, Shenzhen Polytechnic, Shenzhen, 518055, China

[d] Department of Chemistry, Cape Breton University 1250 Grand Lake Road Sydney, Nova Scotia, B1P 6L2, Canada

[e] Department of Biology, University of Waterloo, Waterloo, Ontario, N2L 3G1, Canada

[*]Corresponding authors: linsujing@szpt.edu.cn; xu_zhang@cbu.ca (X.Z.)

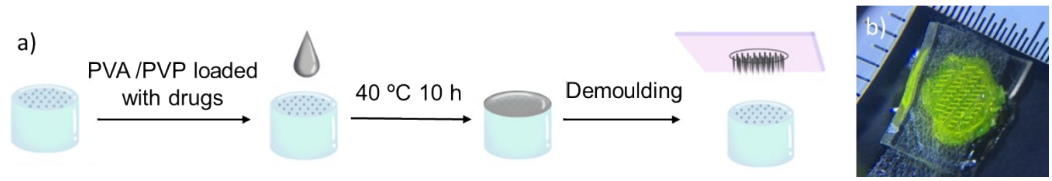

Figure S1. a) Microneedle patch fabrication procedure. b) A microneedle patch containing FITC.

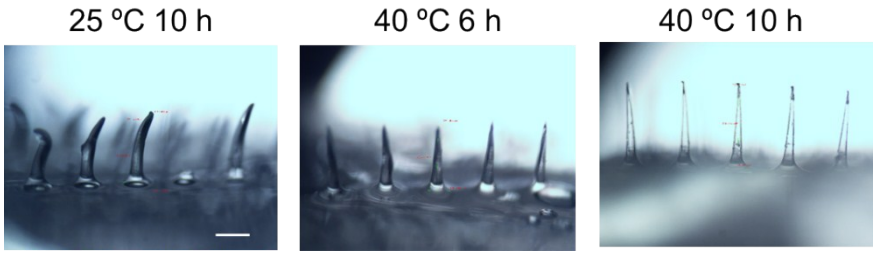

Figure S2. Microneedles formed under different polymerization conditions. Scale bar: 500 µm.

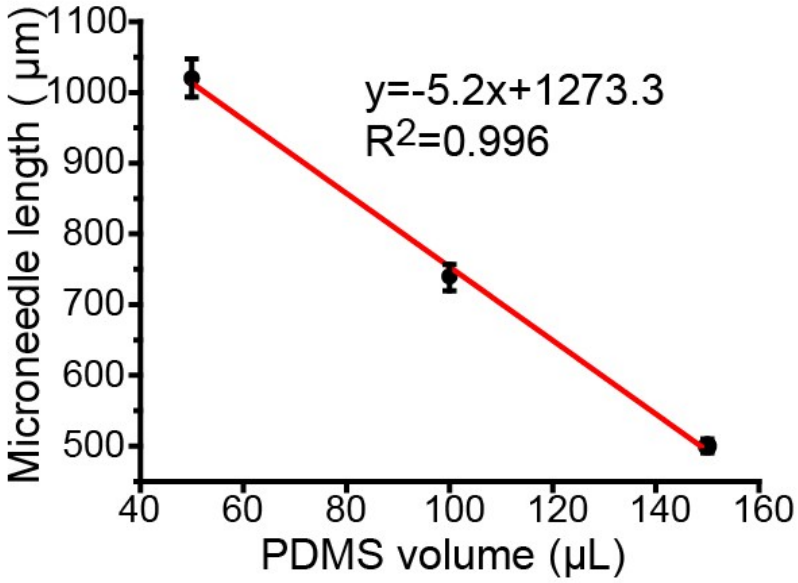

Figure S3. The MN length as a function of the spacer volume. Error bars represent the standard deviation (SD) for *n*=5.

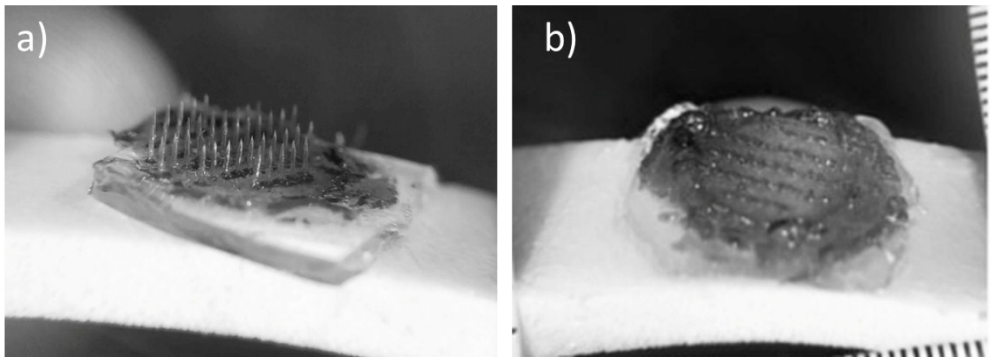

Figure S4. The digital images of the MNs a) before and b) after inserting into skin for 15 min of in vitro permeation experiment.

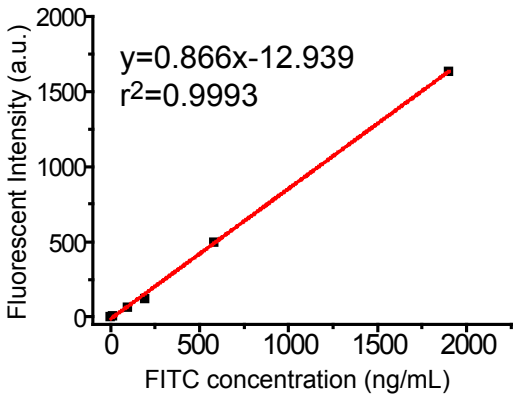

Figure S5. The standard curve of FITC solution using a plate reader.

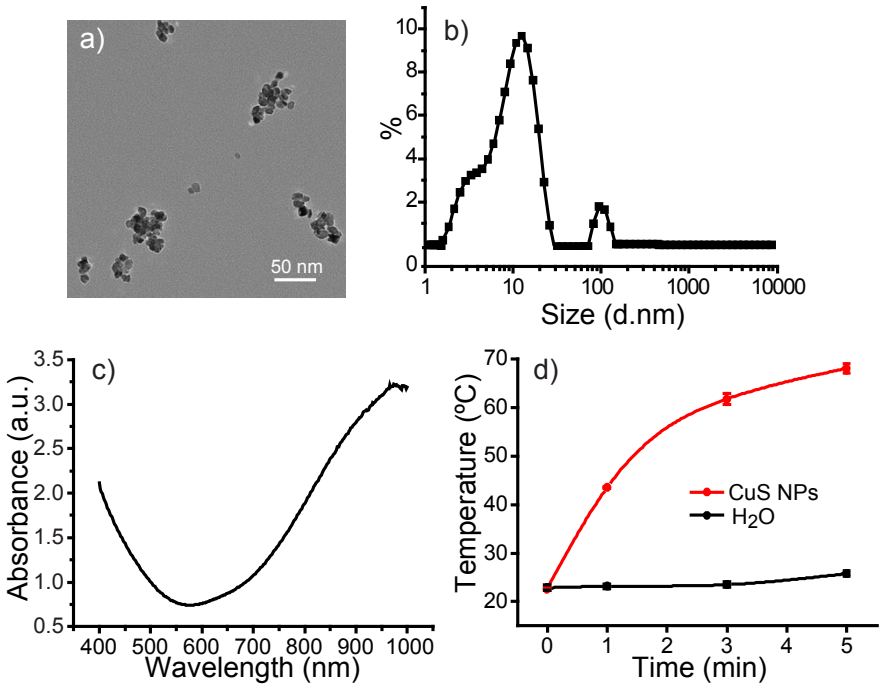

Figure S6. Characterization of the CuS NPs synthesized for photothermal therapy. a) TEM image of CuS NPs. b) The size (hydrodynamic diameter) distribution of the CuS NPs. c) UV-vis absorption spectra of the CuS NPs. d) The temperature change of the CuS NP solution in a 96-well plate upon laser irradiation (850 nm, 1000 mW) over time, where water without CuS NPs treated with laser irradiation served as the control (*n* = 3).

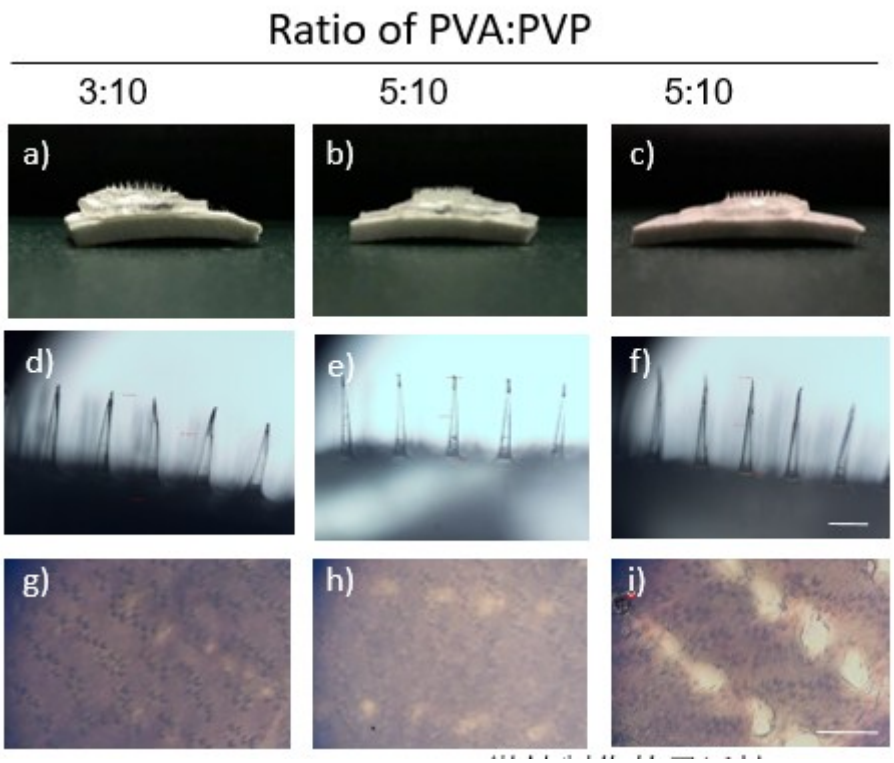

Figure S7. Images and skin insertion properties of microneedle patches with different polymer compositions. a–c) Side view of microneedle patches with different ratio of PVA/PVP, respectively. d–f) Microneedle micrographs of the above compositions. g–i) Mouse skin penetration using the above microneedles. Scale bar: 500 µm.

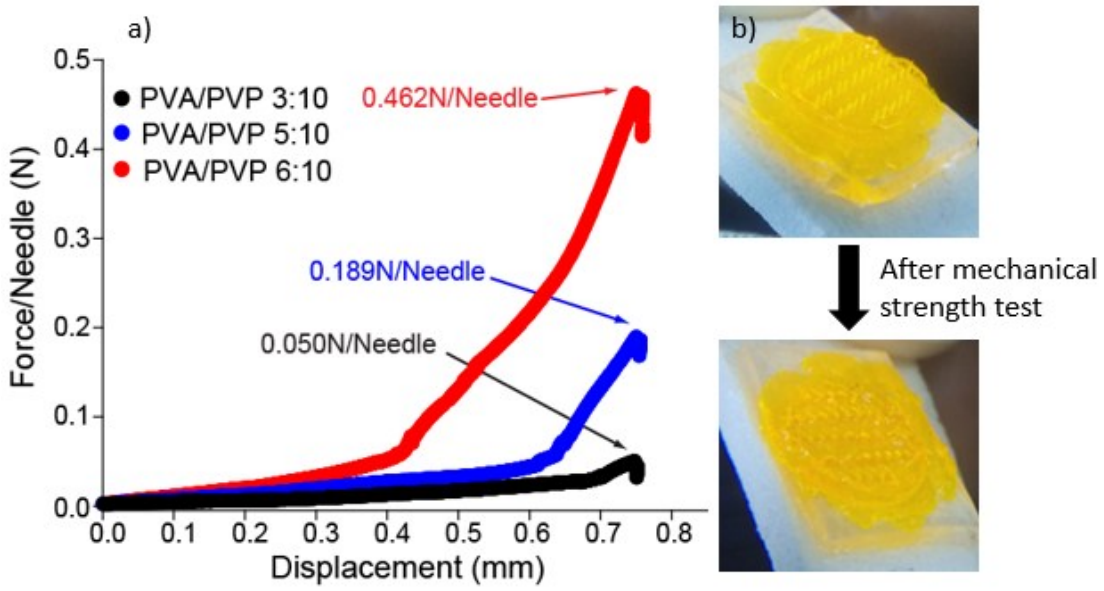

Figure S8. Mechanical behavior of the microneedle patch. a) Mechanical strength (the failure force curves) of the microneedle patches with different PVA/PVP concentrations. b) The images of 30% PVA microneedle before and after the mechanical strength test, showing all microneedles were compressed during the test.